Precision Waveguide System for Measurement of Complex Permittivity of Liquids at Frequencies from 60 to 90 GHz

J. Hunger, I. Cerjak, H. Schoenmaker, M. Bonn, and H. J. Bakker*

FOM Institute AMOLF, Science Park 104,

1098 XG Amsterdam, The Netherlands

Abstract

We describe a variable path-length waveguide setup developed to accurately measure the complex dielectric permittivity of liquids. This is achieved by measuring the complex scattering parameter of the liquid in a waveguide section with a vector network analyzer in combination with an E-band frequency converter. The automated measurement procedure allows fast acquisition at closely spaced intervals over the entire measurement bandwidth: 60-90 GHz. The presented technique is an absolute method and as such not prone to calibration errors. The technique is suited to investigate low loss as well as high loss liquids in contrast to similar setups described previously. We present measurements for a high-loss liquid (water), an intermediate-loss sample (ethanol), and for nearly loss-less *n*-octane. Due to the available phase information the present data have an improved accuracy in comparison with literature data.

* To whom correspondence should be addressed. Electronic mail: bakker@amolf.nl.

I. INTRODUCTION

Measurement of the complex dielectric permittivity at radio, microwave and terahertz frequencies (dielectric spectroscopy) is widely used in many areas of research. It is a common experimental tool to study solids, polymers, liquids and gases. In particular for condensed phase samples, dielectric permittivity spectra can provide valuable insight into the molecular dynamics and interactions.[1,2] By covering a frequency range spanning from several hertz up to terahertz (10^{12} Hz), dynamics on time scales spanning over several orders of magnitude can be investigated. In general, such measurements cannot be performed with a single setup and require several different experimental techniques.

At frequencies below ~ 50 GHz capacitor or coaxial techniques are the best choice due to the wide range of frequencies that can be covered with a single setup. An overview over various measurement geometries can be found in Refs. 3–7. At sub-millimeter and terahertz frequencies, typically 100 GHz and upward, free-space methods are generally preferred.[7,8]

The gap between microwave and terahertz frequencies is of particular interest to study the dipolar dynamics of very common solvents. For instance, the dominant orientational relaxation for water,[9–12] acetone,[13] acetonitrile,[14] or dichloromethane[15] is found between 20 and 80 GHz. Hence, it is vital to cover these frequencies in order to study the dipolar reorientation dynamics of these solvents and their interaction with solutes. For this frequency range neither coaxial lines nor free-space methods provide sufficient accuracy to reliably investigate liquid dynamics,[6,7] and thus guided-wave techniques are required. A technological limitation that persisted for a long time in this frequency range was the lack of phase-sensitive detectors. Hence, considerable experimental effort was required to retrieve the phase change and the attenuation within the sample. This was achieved with interferometry[16,17] or measurements of standing wave ratios[18–20] at a single frequency.

In recent years phase sensitive instrumentation based on waveguide frequency converters in combination with vector network analyzers (VNAs) have become readily available. As a result, complex permittivities can now be obtained from a single measurement of the scattering matrix of a sample in a waveguide.[21–23] However, the positioning of liquids in the waveguide requires windows, which introduce spurious signals. Moreover, the measurement of accurate permittivity data requires a high quality calibration of the instrument and traceable waveguide components. At frequencies above 60 GHz both prerequisites become very

important.[24]

In this paper we present a variable path length waveguide cell, operating at 60 to 90 GHz. The measurements are based on standing wave ratios measured by a vector network analyzer connected to an external WR12 frequency converter (60 - 90 GHz). The technique combines measurements at variable sample thicknesses with state-of-the-art phase-sensitive detection. Using this approach, any bias of the results due to calibration errors or spurious reflections of windows are excluded. We present the results of measurements for loss less (n-octane), intermediate loss (ethanol), and high loss (water) liquids and we compare these to literature values. Owing to the available simultaneous measurements of phase and amplitude, highly accurate data are obtained.

II. DESCRIPTION OF THE SETUP

The experiments are 1-port reflection measurements (S_{11}) using a 4-port VNA (ZVA67, Rhode & Schwarz, Germany) connected to an external E-band frequency converter (ZVA-Z90E, Rhode & Schwarz, Germany) with a dynamic range of > 90 dB. The frequency converter is operated at frequencies, ν, ranging from 60 to 90 GHz and equipped with a WR12 waveguide port using precision flanges. The frequency converter is calibrated with a short/offset-short/match calibration kit, as supplied by the manufacturer. The instrument is connected to the measurement cell via a 90 degree WR12 E-plane band and a WR12-WR15 tapered transition (both Cernex Inc., USA).

Figure 1 shows the measurement cell schematically. The cell is based on a custom WR15 waveguide made from copper and plated with 3 μm of gold. The liquid container within the waveguide is oversized (with respect to the $\nu = 60 - 90$ GHz band) to allow for higher mechanical accuracy.[19] At the bottom of the cell a PTFE window of 0.5 mm thickness is fit into the clearance. The window is slightly oversized to achieve liquid-tight sealing by connecting the flanges. The liquid under investigation is filled from the top and is terminated by a movable, short-circuiting plunger made from gold-plated copper. The plunger can be moved over a total distance of 6 mm using the drive mechanism above the cell. The plunger position is controlled to a relative accuracy of 0.82 % using a computer-controlled DC servo motor actuator (Z812B, ThorLabs, USA).

The measurements were automated using Labview (National Instruments, USA). The

scattering parameters, S_{11}, are recorded with an IF bandwidth of 100 Hz as a function of the plunger position and the frequency at closely spaced intervals. All experiments are performed in a temperature-controlled environment at 25.0 $\pm$ 0.1 °C.

III. THEORY

Assuming a unique mode of propagation (TE_{10}) and a short-circuit reflection at the metal plunger that is independent of the position, the signal reflected by the liquid column in the waveguide is given by[25]

$$S_{11} = \frac{R_1(\nu) + R_2(\nu)\exp(-2\gamma(\nu)x)}{1 + R_3(\nu)\exp(-2\gamma(\nu)x)} \tag{1}$$

where $R_1(\nu)$ $(= \frac{\gamma_0(\nu)+\gamma(\nu)}{\gamma_0(\nu)-\gamma(\nu)})$, $R_2(\nu)$ $(= \frac{1}{r(\nu)})$, and $R_3(\nu)$ $(= \frac{\gamma_0(\nu)+\gamma(\nu)}{(\gamma_0(\nu)-\gamma(\nu))r(\nu)})$ are complex constants and x is the distance of the plunger from an arbitrary reference.[26] $\gamma(\nu)$ $(= \alpha(\nu) + \mathrm{i}\beta(\nu))$ is the complex propagation constant of the liquid with the absorption coefficient, $\alpha(\nu)$, and the phase coefficient, $\beta(\nu)$. $\gamma_0(\nu)$ is the propagation constant of the preceding (empty) waveguide and $r(\nu)$ the complex reflection coefficient at the metal plunger (Figure 2).

The complex permittivity of the material under investigation, $\varepsilon'(\nu) - \mathrm{i}\varepsilon''(\nu)$, with the frequency dependent dielectric permittivity, $\varepsilon'(\nu)$, and the dielectric loss, $\varepsilon''(\nu)$, is related to the propagation constant, $\gamma(\nu)$, in the waveguide via[26]

$$\varepsilon'(\nu) - \mathrm{i}\varepsilon''(\nu) = \left(\frac{c}{\nu}\right)^2 \left(\left(\frac{1}{\lambda_\mathrm{c}}\right)^2 - \left(\frac{\gamma(\nu)^2}{2\pi}\right)^2\right) \tag{2}$$

In Eq. 2 c is the speed of light *in vacuo*, and λ_c $(= 2a)$ is the limiting wavelength for propagation of the TE_{10} mode in a waveguide of width a.

We modeled the measured $S_{11}(x)$ values by simultaneously fitting the modulus and the phase to the experimental data to Eq. 1 at each frequency. Non-linear least-square optimizations were performed using a direct simplex algorithm[27] implemented in Matlab (MathWorks, USA). From the propagation constant $\gamma(\nu)$ thus obtained, we calculate the frequency dependent complex permittivity according to Eq. 2. The permittivity values of three independent measurements are averaged and we assume the error to correspond to the standard deviation within the three measurements.

IV. RESULTS

We measured data for water ($> 99.99\,\%$, HPLC-grade, Sigma-Aldrich), ethanol ($> 99.8\,\%$, analytical grade, Sigma-Aldrich), and *n*-octane ($> 99\,\%$, anhydrous, Sigma-Aldrich) at 25 °C. In Figure 3 exemplarily measured values of S_{11} at 80 GHz are depicted for the three liquids. For water the electromagnetic wave is completely attenuated in the sample after a single oscillation of the field, and at $x \gtrsim 1\,\text{mm}$ the measured signal is formed only by the signal reflected at the window-sample interface. For ethanol the signal reflected from the plunger contributes for longer x and the measured reflection coefficient follows a damped oscillation. For the loss-less sample *n*-octane no attenuation can be detected within the experimental accuracy. As can be seen in Figure 3, Eq. 1 reproduces the measured reflection coefficients very well except for $|S_{11}|$ obtained for the loss-less sample *n*-octane (as will be discussed below). The average deviations of the experimental values of $|S_{11}|$ and $\phi(S_{11})$ from the fitted curves obtained using Eq. 1 are $0.06\,\%$ for water, $0.26\,\%$ for ethanol, and $7.5\,\%$ for *n*-octane, relative to the maximum range of S_{11}.

In Figure 4 we show the complex permittivities obtained from the measurements of S_{11} at different frequencies. These complex permittivities are obtained using Eq. 2. The dielectric permittivities, $\varepsilon'(\nu)$, and the dielectric losses, $\varepsilon''(\nu)$, vary smoothly with frequency. In general, the precision is found to be very high, except for the loss-less liquid *n*-octane, for which the reproducibility is slightly worse than for the other samples. This can be traced back to the deviations of the experimental $|S_{11}|$ and the fitted $|S_{11}|$ of Eq. 1 (Figure 3).

In Figure 4 the obtained complex permittivities are also compared to available literature values. It is noteworthy, that all reported literature values solely rely on measurements of the amplitude of the electromagnetic waves and that phase information was lacking. Further, only a limited number of frequencies was investigated due to technological limitations.

For water, which is probably the most extensively studied solvent,[11,28] the values reported here are in excellent agreement with the literature values. However, as can be seen in Figure 4, the scatter in the literature data is significantly higher than for the present measurements. Further, relaxation models[10–12] describing the dielectric properties of water, which are based on measurements over a broader frequency range, differ among themselves (Figure 4). It is noteworthy, that the model reported by Buchner *et al*[10] is in excellent agreement with our values (average relative deviation better than $1.3\,\%$), while the ε' values recommended by

Ellison[11] and Kaatze[12] are somewhat higher and lower, respectively.

In the case of ethanol, reports of complex permittivities are scarce and to the best of our knowledge only one group has previously reported measurements in the frequency range $60 - 90\,\mathrm{GHz}$ at $25\,^{\circ}\mathrm{C}$. This study[9] is in reasonable agreement with our values, though the reported dielectric loss values are somewhat lower than our results. Also the reported model is somewhat different from our values.[9] However, our data are in excellent agreement (average relative deviation better than $0.4\,\%$) with a more recent model for ethanol reported by the same group in Ref. 29.

As will be discussed below, it is difficult to obtain accurate values for the complex permittivity at frequencies of the present study for low permittivity or loss-less samples without phase information. As a result, no complex permittivity data are reported in the literature for *n*-octane at frequencies between 60 and 90 GHz. However, the present results can be compared to the static permittivity ($\varepsilon_{\mathrm{stat}} = \varepsilon'(\nu \to 0)$). The present average value of $\varepsilon' = 1.91 \pm 0.01$ is slightly smaller than the static value of $\varepsilon_{\mathrm{stat}} = 1.94$,[32] probably due to a small dispersion in ε' for *n*-octane in the frequency range $\nu = 0 - 60\,\mathrm{GHz}$.

V. DISCUSSION

The described technique yields very precise complex permittivity values. The average reproducibility in determining ε' and ε'' within three independent measurements better than ± 0.1 (Figure 4). We note that at some particular frequencies the statistical variation is larger. This is very likely due to some resonances in the equipment. The high precision indicates that instabilities in the setup are negligible. The losses within the surface of the waveguide are minimized by gold-plating the custom made waveguide. It was shown previously[30] that these losses have a negligible effect at distances relevant for the present setup ($x < 6\,\mathrm{mm}$). Further, the precise mount of the axle and the drive mechanism assure accurate positioning of the plunger. This warrants a constant reflection coefficient, r, at the gold-plated metal plunger.

It is apparent from Figure 3 that Eq. 1 excellently describes the measured S_{11} values for water and ethanol. For *n*-octane somewhat higher deviations of the experimental values are observed. This can be explained by the finite thickness of the window containing the sample in the waveguide. More specifically, in Eq. 1 only the transition from the sample to the empty

waveguide section is included, i.e. the window is assumed to be infinitely thin. Attempts to include the finite thickness[31] of the window in Eq. 1 were not successful. The magnitude of the signal reflected at each interface is determined by the difference in the propagation of both media. For high permittivity samples (ethanol and water) the difference between air and teflon is negligible compared to the difference between teflon and the sample. Hence, the latter interface is dominating the measured standing-wave ratio and the contribution of the air-teflon transition is negligible. For the low permittivity sample *n*-octane both transitions become comparable which leads to another interference effect resulting in the additional minima of $|S_{11}|$ for *n*-octane (Figure 3). However, the total recorded signal is dominated by the reflection at the metal plunger and, thus, owing to the availability of the phase information, the complex permittivity of low permittivity, low-loss samples can be accurately determined with the present method.

The good agreement of the experimental S_{11} values with the fit using Eq. 1, that is based on propagation of the TE_{10} mode, indicates that higher order modes do not contribute significantly to the recorded scattering parameter. In particular for high-permittivity samples like water, higher order modes can propagate in the waveguide section containing the sample, but the present data do not evidence the presence of these higher-order modes.

The described method makes use of the relative measurement of S_{11} as function of relative sample thickness to determine complex permittivities. Hence, it is an absolute method[5] and not sensitive to errors introduced due to non-reproducible flange connections of the waveguide. Further, it does not require an accurate calibration for directivity, frequency response, and source match error terms. This is particularly important at mm and sub-mm wavelengths, where fabrication of precise waveguide calibration standards is problematic.[24]

VI. CONCLUDING REMARKS

We present a variable path-length waveguide reflection cell for accurate measurement of complex permittivities of liquid samples at 60 to 90 GHz. Making use of a state-of-the-art vector network analyzer allows fast measurement of complex permittivities at closely spaced intervals over the entire bandwidth of the waveguide setup. The high number of data points gives significant statistics and is not prone to systematic errors specific to single frequencies. The described technique is an "absolute" method and does not require any calibration.

This is achieved by measuring S_{11} as function of relative sample thickness. In contrast to single-point measurements for fixed sample geometries in transmission or reflection geometry, systematic errors due to reflections at windows can be excluded. The determination of the complex permittivity is based on the magnitude and the phase information, in contrast to techniques described previously.[16–20] As a consequence the complex permittivities values are determined with an improved accuracy. Further, the phase sensitivity provides applicability of our instrumentation to a wide range of liquids, ranging from nearly loss less to high loss samples.

Acknowledgment

This work is part of the research program of the *Foundation for Fundamental Research on Matter (FOM)*, which is part of the *Netherlands Organisation for Scientific Research (NWO)*. JH thanks the *Deutsche Forschungsgemeinschaft* (DFG) for funding through the award of a research fellowship.

[1] F. Kremer and A. Schönhals, eds., *Broadband Dielectric Spectroscopy* (Springer, Berlin, 2003).

[2] P. Debye, *Polar Molecules* (Dover, New York, 1930).

[3] J. Baker-Jarvis, M. D. Janezic, B. F. Riddle, R. T. Johnk, P. Kabos, C. L. Holloway, R. G. Geyer, and C. A. Grosvenor, Tech. Rep., NIST Technical Note 1536 (2004).

[4] A. P. Gregory and R. N. Clarke, IEEE Trans. Dielectr. Electr. Insul. **13**, 727 (2006).

[5] U. Kaatze and Y. Feldman, Meas. Sci. Technol. **17**, R17 (2006).

[6] *A guide to the characterization of dielectric materials at rf and microwave frequencies*, The Institute of Measurement and Control (IMC) and The National Physical Laboratory (NPL), London, ISBN 0 904457 38 9 (2003).

[7] J. Krupka, Meas. Sci. Technol. **17**, R55 (2006).

[8] C. A. Schmuttenmear, Chem. Rev. **104**, 1759 (2004).

[9] J. Barthel, K. Bachhuber, R. Buchner, and H. Hetzenauer, Chem. Phys. Lett. **165**, 369 (1990).

[10] R. Buchner, J. Barthel, and J. Stauber, Chem. Phys. Lett. **306**, 306 (1999).

[11] W. J. Ellison, J. Phys. Chem. Rev. Data **36**, 1 (2007).

[12] U. Kaatze, J. Chem. Eng. Data **34**, 371 (1989).

[13] J. K. Vij and Y. P. Kalmykov, J. Chem. Phys. **99**, 2506 (1993).

[14] R. Jellema, J. Bulthuis, and G. van der Zwan, J. Mol. Liq. **73-74**, 179 (1997).

[15] J. Hunger, A. Stoppa, A. Thoman, M. Walther, and R. Buchner, Chem. Phys. Lett. **471**, 85 (2009).

[16] J. Barthel, K. Bachhuber, R. Buchner, H. Hetzenauer, and M. Kleebauer, Ber. Bunsen–Ges. Phys. Chem. **95**, 853 (1991).

[17] U. Kaatze, R. Pottel, and A. Wallusch, Meas. Sci. Technol. **6**, 1201 (1995).

[18] S. Szwarnowski and R. J. Sheppard, J. Phys. E: Sci. Instrum. **10**, 1163 (1977).

[19] M. G. M. Richards and R. J. Sheppard, Meas. Sci. Tech. **2**, 663 (1991).

[20] K. E. Mattar and H. A. Buckmaster, Meas. Sci. Technol. **2**, 891 (1991).

[21] B.-K. Chung, Progress In Electromagnetics Research **75**, 239 (2007).

[22] Y. Wang and M. N. Afsar, Progress In Electromagnetics Research **42**, 131 (2003).

[23] U. C. Hasar, Progress In Electromagnetics Research **107**, 31 (2010).

[24] C. Oleson and A. Denning, 56th ARFTG Conference Digest-Fall pp. 1–9 (2000).

[25] A. R. von Hippel, *Dielectrics and Waves* (John Wiley & Sons, Inc., New York, 1954).

[26] R. Van Loon and R. Finsy, Rev. Sci. Instrum. **44**, 1204 (1973).

[27] J. C. Lagarias, J. A. Reeds, M. H. Wright, and P. E. Wright, SIAM Journal of Optimization **9**, 112 (1998).

[28] W. J. Ellison, K. Lamkaouchi, and J. M. Moreau, J. Mol. Liq. **68**, 171 (1986).

[29] T. Sato and R. Buchner, J. Phys. Chem. A **108**, 5007 (2004).

[30] R. Van Loon and R. Finsy, Rev. Sci. Instrum. **45**, 523 (1974).

[31] J. D. Cutnell, D. E. Kranbuehl, E. M. Turner, and W. E. Vaughan, Rev. Sci. Instrum. **40**, 908 (1969).

[32] D. R. Lide, ed., *CRC–Handbook of Chemistry and Physics* (CRC–Press, Boca Raton, USA, 2004), 85th ed.

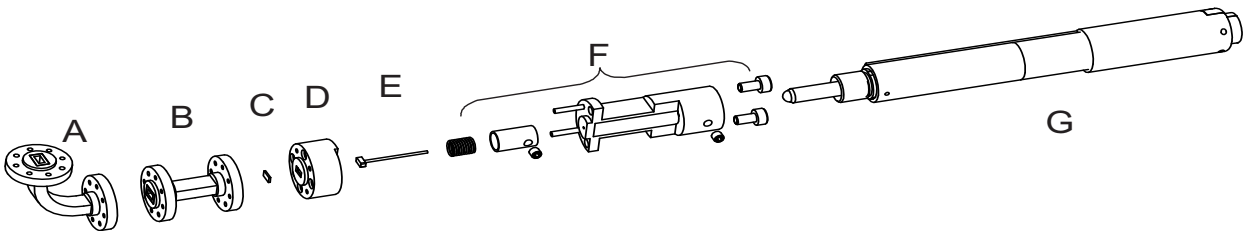

FIG. 1: Schematic representation of the sample cell. A: E-plane bend; B: WR12-WR15 tapered transition; C: PTFE window; D: sample containing custom waveguide; E: short-circuiting plunger; F: drive mechanism; G: motor actuator.

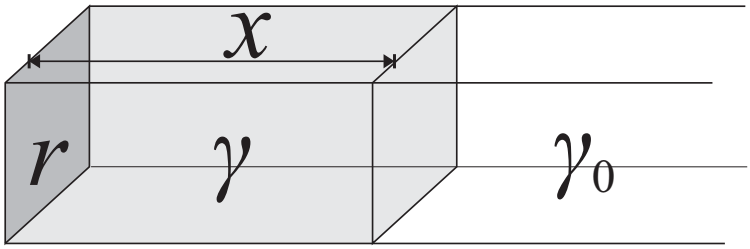

FIG. 2: Schematic representation of the quantities underlying Eq. 1. The sample is contained in a waveguide of length x with a propagation coefficient γ. The sample is terminated with a short-circuiting metal plunger with complex reflection coefficient r. The preceding, empty section has a propagation constant γ_0.

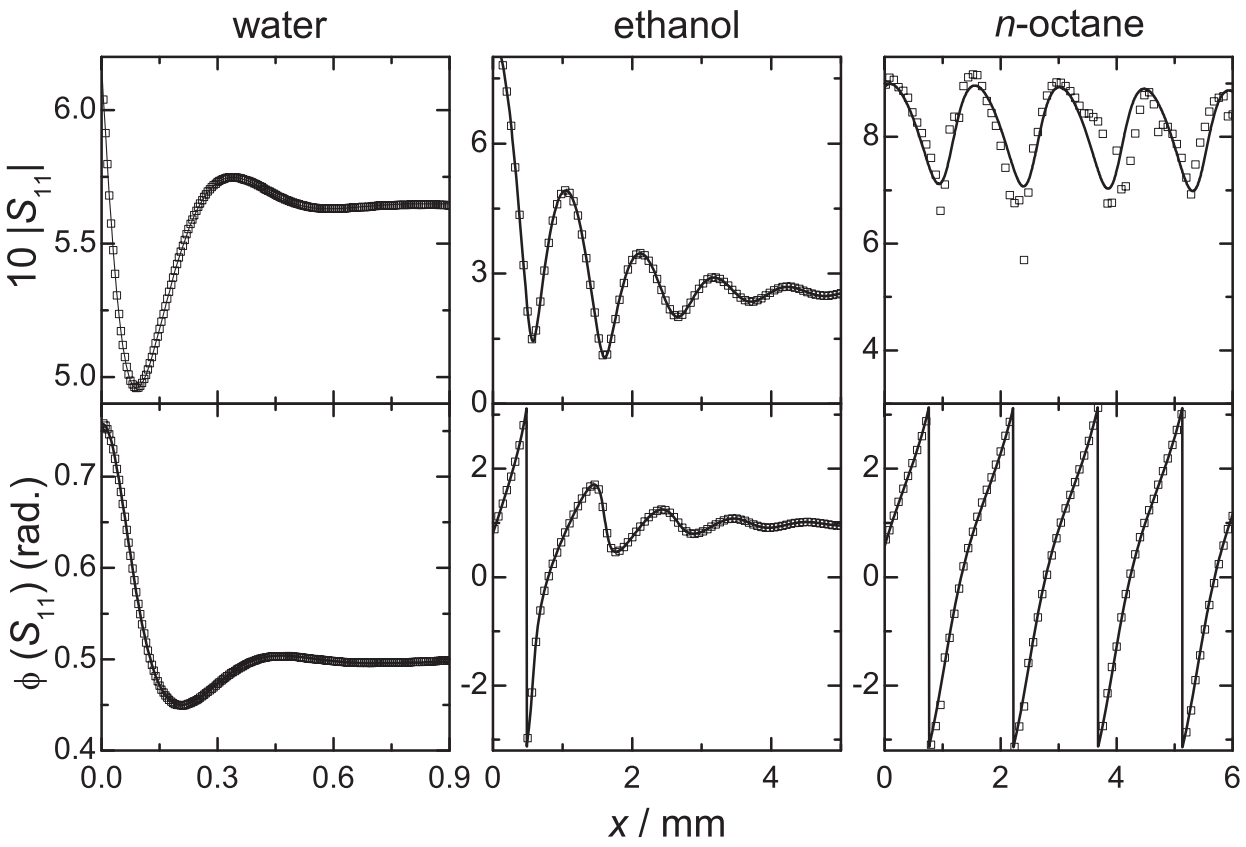

FIG. 3: Modulus, $|S_{11}|$, and phase, $\phi(S_{11})$, of the reflected signal at $\nu = 80\,\mathrm{GHz}$ as a function of plunger position, x, for water, ethanol, and n-octane. The symbols correspond to experimental data, the lines show the fits to Eq. 1.

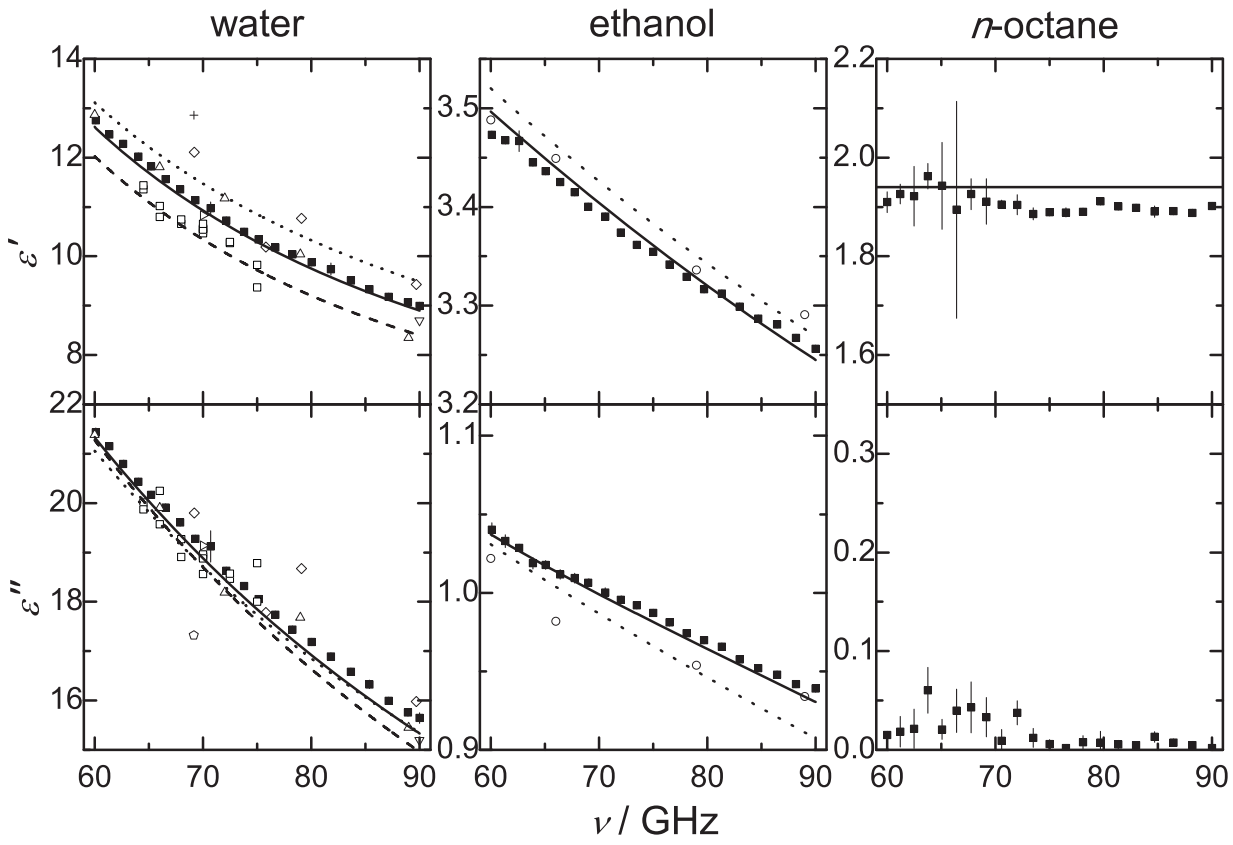

FIG. 4: Dielectric permittivity, $\varepsilon'(\nu)$, and loss, $\varepsilon''(\nu)$, spectra for water, ethanol, and n-octane (■). Only 21 out of 201 data points are displayed for visual clarity. The error bars represent the standard deviation within three independent measurements. Open symbols represent literature values for ethanol taken from Ref. 9 and water as summarized in Ref. 28 at 25 °C. Lines correspond to relaxation models for water reported by Buchner *et al.*[10] (solid line), Ellison[11] (dotted line), and Kaatze[12] (dashed line). Models for ethanol according to Buchner *et al.*[9] (dotted line), and Sato and Buchner[29] (solid line) are also included. For n-octane the solid line represents the static permittivity of n-octane at 25 °C.[32]